

Anomalous Isothermic Enthalpy of Adsorption of Methane on Zeolite-Templated Carbon

Nicholas P. Stadie,* Maxwell Murialdo, Channing C. Ahn, and Brent Fultz

W. M. Keck Laboratory, California Institute of Technology, 138-78, Pasadena, California 91125, United States

S Supporting Information

ABSTRACT: A thermodynamic study of the enthalpy of adsorption of methane on high surface area carbonaceous materials was carried out from 238 to 526 K. The absolute quantity of adsorbed methane as a function of equilibrium pressure was determined by fitting isotherms to a generalized Langmuir-type equation. Adsorption of methane on zeolite-templated carbon, an extremely high surface area material with a periodic arrangement of narrow micropores, shows an increase in isothermic enthalpy with methane occupancy; i.e., binding energies are greater as adsorption quantity increases. The heat of adsorption rises from 14 to 15 kJ/mol at near-ambient temperature and then falls to lower values at very high loading (above a relative site occupancy of 0.7), indicating that methane/methane interactions within the adsorption layer become significant. The effect seems to be enhanced by a narrow pore-size distribution centered at 1.2 nm, approximately the width of two monolayers of methane, and reversible methane delivery increases by up to 20% over MSC-30 at temperatures and pressures near ambient.

High-pressure adsorption is vital to numerous engineering processes and industrial applications today, and perhaps relevant to future systems for compact storage of methane and hydrogen fuels.¹ Carbonaceous sorbent materials are particularly attractive because they are lightweight, abundantly available, and simple to produce and can effectively increase the volumetric density of stored gases.^{2–4} For effective energy storage by physical adsorption, a high total capacity (corresponding to a large number of binding sites) is necessary for high potential delivery. Additionally, the characteristic binding energies of the sorbent/adsorbate interactions are crucial to the practical deliverable capacity because the storage tank must be cycled between two finite pressures, and the amount stored in the system at the lower bound (e.g., 0.3 MPa) should be low. The optimal material for physisorptive energy storage is assumed to have a high binding energy that is constant with increased loading. For H₂, the average enthalpy of adsorption across a wide variety of carbon materials (activated carbon, nanofibers, aerogels, templated carbons, etc.) is 4–6 kJ (mol H₂)⁻¹,⁵ not significantly higher than the average thermal energy at 298 K and limits their effective use to cryogenic temperatures. Physical adsorption of methane is much stronger, typically 12–20 kJ/mol, and near-ambient-temperature applications for methane storage are more promising.

In microporous carbonaceous materials, pore structure and surface chemistry offer the potential to adjust the thermodynamic properties of adsorption. Boron- and nitrogen-doped materials show promise in exhibiting higher enthalpies of adsorption of H₂,^{6–8} but as in pure carbon-based materials, the enthalpy declines with loading. A more effective approach for tuning the thermodynamics of adsorption is by controlling the pore-size distribution and mean pore width to achieve optimal binding interactions.⁹ Theoretical models of adsorption in graphitic slit pores show that pore widths corresponding to three molecular diameters of the adsorptive gas are ideal for maximizing adsorbate/adsorbate interactions and increasing the total energy of adsorption.^{10–12} However, adsorption measurements on engineered graphene scaffolds¹³ and other microporous materials^{14,15} have never shown an appreciably increasing binding energy in the high surface coverage regime.

Template carbonization is an effective technique for producing carbonaceous materials with exceptionally large specific surface area and controlled porosity.¹⁶ Zeolite-templated carbons (ZTCs) are microporous, amorphous carbon materials with extremely high surface area and a periodic array of pores complementary to the structure of the zeolite used in the template carbonization synthesis. The H₂ storage capacities of ZTCs were reported to be exceptionally high at pressures between 10 and 34 MPa,¹⁷ but recent results^{18,19} showed that this capacity is simply proportional to specific surface area, typical of other materials.^{2,3}

The nature of the microstructure of carbonaceous materials has not been reported to have an effect on their adsorptive capacities for methane, but pore widths in these materials do approach the optimal value, suggested to be 1.14 nm.^{10,11} Recent calculations of methane adsorption on metal/organic framework CPO-27-Mg, a crystalline material with well-characterized adsorption sites within small (~1.1 nm) cages, show that strong adsorbate/adsorbate interactions play an important role in the enthalpy, resulting in a 15% increase in excess capacity near 298 K.²¹ The average binding energy, though, decreases with loading due to the sequential filling of binding sites corresponding to distinct, decreasing energies. Materials with controlled pore widths⁹ such as templated carbons offer the potential for a more homogeneous distribution of sorption sites, but to date a material with constant isothermic enthalpy has been elusive.

Here we investigate high-pressure methane sorption in ZTC-3, a model zeolite-templated carbon material for methane storage, with a narrow pore-size distribution centered at 1.2 nm.

Received: November 20, 2012

Published: December 23, 2012

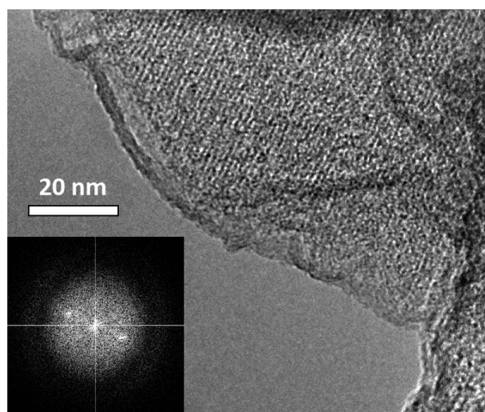


Figure 1. TEM micrograph of ZTC-3 confirming a pore-to-pore periodicity of 1.0 nm, and the Fourier transform of the image (inset).

ZTC-3 was synthesized by impregnating zeolite NaY with polyfurfuryl alcohol, undergoing a propylene CVD step at 700 °C, and carbonization was performed at 900 °C. The template was removed by dissolution in HF. Details of the synthesis, and the important steps for attaining high template fidelity, are reported elsewhere.¹⁸ For comparison, two other commercial activated carbons were also investigated: CNS-201, a modest surface area carbon with extremely narrow micropores, and MSC-30, a superactivated carbon with extremely high surface area that is often measured as a standard. These materials were degassed at 250 °C under vacuum to <0.1 mPa before use.

Nitrogen adsorption/desorption isotherms at 77 K were collected to calculate surface areas, micropore volumes, and pore-size distributions of the materials. The Brunauer–Emmett–Teller (BET) surface areas of CNS-201, MSC-30, and ZTC-3 are 1095, 3244, and 3591 m²/g, respectively. The Dubinin–Radushkevich method was used to calculate their microporous volumes: 0.45, 1.54, and 1.66 mL/g. The pore-size distribution in CNS-201, obtained by the nonlocalized density functional theory (NLDFT) method, contains three peaks, at 0.54, 0.80, and 1.18 nm, with 50%, 20%, and 15% of the pore volume in each, respectively. MSC-30 contains a broad distribution of pore widths between 0.6 and 3.5 nm, and 40% of the pore volume is contained in pores >2.1 nm in width. The distribution of pores in ZTC-3 is characterized by a single sharp peak centered at 1.2 nm, with >90% of the pore volume having a pore width between 0.85 and 2.0 nm. This regularity of pore size in ZTC-3 was confirmed by X-ray diffraction with Cu K α radiation, showing a sharp peak centered at $2\theta = 6^\circ$, and transmission electron microscopy, showing a periodic spacing of diffraction contrast corresponding to pores of width 1 nm (see Figure 1).

Skeletal densities of the samples were measured by helium pycnometry; the activated carbons have 2.1 g/mL, consistent with a wide variety of carbonaceous materials,³ while ZTC-3 has a lower skeletal density (1.8 g/mL, consistent with other ZTCs¹⁷), presumably due to increased hydrogen terminations (see Supporting Information (SI)).

Methane adsorption isotherms at all temperatures were measured with a volumetric Sieverts apparatus, commissioned and verified for accurate measurements up to 10 MPa.^{22–24} Two adsorption runs using research-grade methane (99.999%) were performed at each temperature, and the data were combined for thermodynamic analysis. Multiple adsorption/desorption cycles were also performed at various temperatures to ensure full reversibility of methane physisorption in the complete temper-

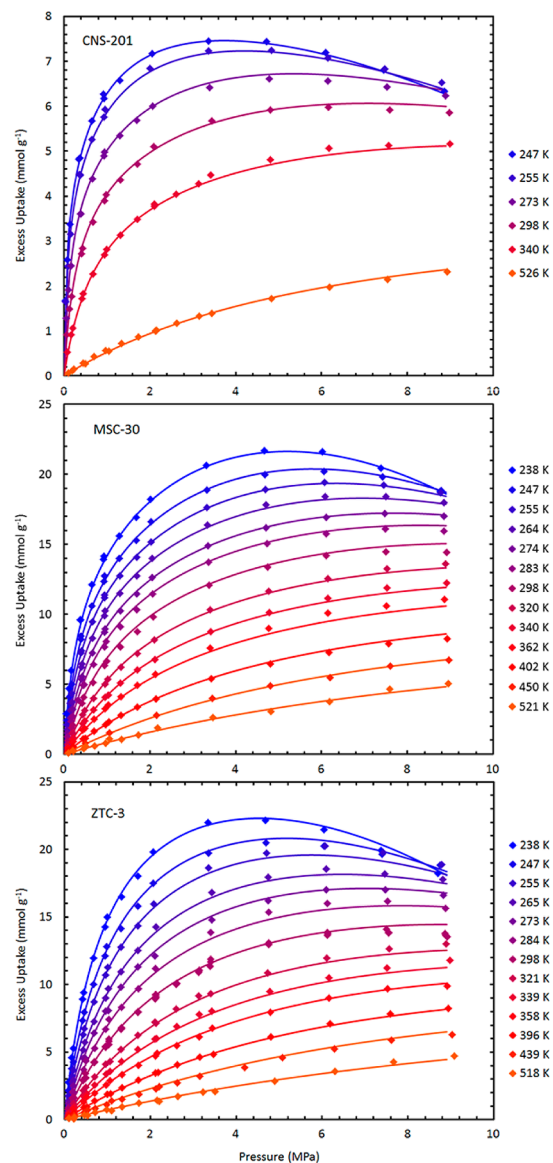


Figure 2. Equilibrium excess adsorption isotherms of methane on CNS-201, MSC-30, and ZTC-3 between 0 and 9 MPa at all temperatures measured: experimental data (diamonds) and fitted results (lines).

ature and pressure regime of study and to test the precision of the experiments. Error between cycles is <1% of the measured value.

Equilibrium adsorption isotherms of methane are shown in Figure 2. The experimental quantity of adsorption is the Gibbs surface excess, the amount of adsorbate in excess of the gas density within the entire void volume of the container; hence, the adsorption shows a surface excess maximum at high pressures. This maximum is a readily accessible figure of merit for the gravimetric performance of a material at a fixed temperature. The excess maximum is similar for ZTC-3 and MSC-30 at room temperature, but slightly higher for MSC-30: 14.5 mmol/g at 8 MPa. While excess adsorption increases faster for MSC-30 at pressures between 0 and 0.8 MPa, uptake in ZTC-3 increases fastest between 0.8 and 5.7 MPa. Gravimetric uptake in CNS-201 is substantially less at all temperatures due to its low specific surface area. The highest measured excess uptake of this study is for ZTC-3 at 238 K: 22.1 mmol/g (26.2 wt%) at 4.7 MPa, despite a gentler initial increase at low pressure. Interestingly, the excess uptake in ZTC-3 is also greater than for MSC-30 at high

temperatures, although neither reaches a maximum between 0 and 9 MPa. At all temperatures, methane uptake in ZTC-3 is characterized by a gradual initial rise and delayed increase at pressures between 0.2 and 2 MPa, leading to higher eventual methane capacity than MSC-30, a material of comparable specific surface area.

For thermodynamic calculations, interpolation of the data of Figure 2 is necessary. It is common to proceed with the measured Gibbs excess quantities approximating the actual (absolute) adsorbed amount, an acceptable practice for studies of adsorption well below the critical point (low pressure and temperature) where excess and absolute adsorption quantities are approximately equal. At temperatures and pressures near the critical point and above, however, thermodynamic calculations from excess adsorption data lead to well-documented errors,²⁵ and quantities calculated by this method should be referred to as “isoexcess” quantities.²⁶ A detailed investigation of the effects of different analysis methods of the data acquired in this study is given in the SI and elsewhere.²⁷

The Gibbs definition of the surface excess quantity, n_e , depends on the bulk gas density, ρ , as

$$n_e = n_a - V_{\text{ads}} \rho(P, T)$$

To calculate the absolute adsorbed quantity, n_a , the remaining unknown is the volume of the adsorption layer, V_{ads} , and numerous methods have been suggested to estimate it.^{25,28–32} A general approach is to let the adsorption volume be an independent parameter of the fitting equation. We adopted the following fitting equation for Gibbs excess adsorption, n_e , as a function of pressure, P , and temperature, T , where V_{ads} scales with coverage up to a maximum, V_{max} :

$$n_e(P, T) = (n_{\text{max}} - V_{\text{max}} \rho(P, T)) \left(\sum_i \alpha_i \left(\frac{K_i P}{1 + K_i P} \right) \right)$$

$$K_i = \frac{A_i}{\sqrt{T}} e^{E_i/RT} \quad \sum_i \alpha_i = 1$$

A generalized Langmuir equation (as above) requires a relatively small number of fitting parameters to achieve a satisfactory fit to the experimental data.^{25,33} The minimum number of independent parameters is desired, and we find that $i = 2$ yields satisfying results across a large number of materials in supercritical adsorption studies of both methane and H_2 adsorption on carbon.

The maximum in excess adsorption measured in this study at 298 K scales linearly with the specific surface area of the materials studied, a relationship analogous to “Chahine’s rule”⁴ for the surface excess maximum of H_2 at 77 K, consistent with the reported linear trend for methane uptake at 3.5 MPa and 298 K.²⁰ The fit parameters also generally correlate with the properties of the materials studied. The scaling parameter n_{max} is proportional to the number of binding sites and is well approximated by the BET specific surface area. The maximum volume of the adsorbed layer, V_{max} , is also proportional to surface area for the activated carbons, but is limited (in the case of ZTC-3) by the pore width, a direct result of complete pore filling since this material has both molecular-sized pores and extremely high microporosity. The maximum volume of the adsorbed layer in ZTC-3, if taken to be proportional to surface area, corresponds to half of the mean pore diameter of the material: a thickness of 0.6 nm.

The thermodynamic quantity of interest for adsorbent materials is the differential enthalpy of adsorption,³⁴ ΔH_{ads} ,

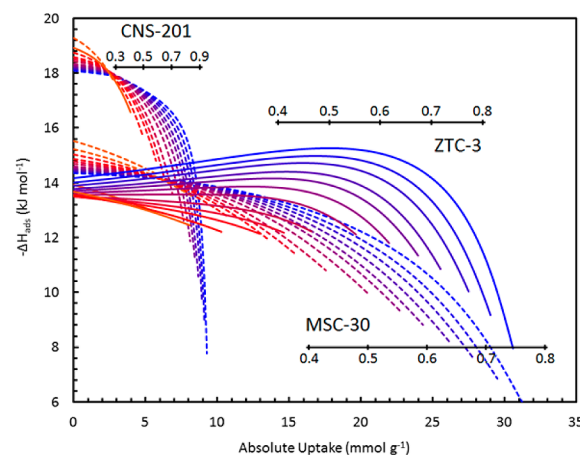


Figure 3. Isosteric enthalpy of methane adsorption on CNS-201, MSC-30, and ZTC-3 from 238 to 523 K (color indicates the temperature from low to high as blue to red). Scale bars of the fractional site occupancy, θ (specific to each material), are inset.

often obtained by the isosteric method and reported as the positive value q_{st} , the isosteric heat of adsorption (in this work, “enthalpy” refers to the positive value):³⁵

$$q_{\text{st}} = -\Delta H_{\text{ads}}(n_a) = -T \left(\frac{\partial P}{\partial T} \right)_{n_a} (\Delta v_{\text{ads}})$$

It is necessary to use this general form of the Clausius–Clapeyron relationship for methane adsorption at high pressure because of the significant non-ideality of methane gas-state properties. Its derivation and explanation with respect to the usual ideal-gas form of the equation are given in the SI. The only simplifying assumption made in this work is that the net change in molar volume of the system upon adsorption, Δv_{ads} , is approximately equal to that of the difference between the bulk gas and liquid methane. Variations on this approximation had little effect on the result. A modified Webb–Benedict–Rubin equation of state was used to calculate the bulk gas density, giving significantly different results than by assuming ideal gas density. The isosteric enthalpy of methane adsorption on CNS-201, MSC-30, and ZTC-3 is shown in Figure 3.

The Henry’s law value of adsorption enthalpy, ΔH_0 , is calculated by extrapolating the enthalpy of adsorption to zero pressure. The Henry’s law values for CNS-201, MSC-30, and ZTC-3 are 18.1–19.3, 14.4–15.5, and 13.5–14.2 kJ/mol, respectively. The temperature dependence of ΔH_0 for CNS-201 and MSC-30 is the same: +4.1 J/mol·K. The Henry’s law values from 238 to 518 K for ZTC-3 depend nonlinearly on temperature, indicating significantly different thermodynamics of methane adsorption in this range. At low temperatures the trend is negative (–16 J/mol·K at 247 K), and then increases toward that of the activated carbons (reaching +3.0 J/mol·K at 450 K).

The characteristics of methane adsorption as a function of fractional site occupancy, θ , in the activated carbons (CNS-201 and MSC-30) are typical of other carbon materials, with q_{st} decreasing with θ . In the range $0 < \theta < 0.6$, the more graphitic CNS-201 shows a more gradual decrease of q_{st} than MSC-30, indicative of more heterogeneous site energies in the latter. Surprisingly, the isosteric enthalpy of adsorption in ZTC-3 increases to a maximum at $\theta = 0.5$ – 0.6 at temperatures from 238 to 273 K. The enthalpy then declines rapidly at high coverage. Beyond $\theta = 0.7$, the rapid decline is similar in all three materials due to very high density in the high-pressure gas.

The increasing isosteric enthalpy of adsorption in ZTC-3 is anomalous compared to previous experimental reports of methane adsorption on carbon. The increase of 1.1 kJ/mol at 238 K is an increase of 8%, a large effect. It is likely that this originates with intermolecular interactions between adsorbed methane molecules, as suggested by theoretical work.^{14,21,36} For gaseous methane, the chemical potential does not increase so rapidly with pressure as for an ideal gas, a characteristic of attractive intermolecular interactions. At intermediate θ , the adsorbed methane molecules may find surface configurations that optimize intermolecular interactions. The average distance between adsorbed methane molecules (approximated as the square root of the BET surface area per molecule) at the surface excess maximum was the same in all three materials in this study (e.g., 0.5 nm at 238 K), so the more attractive interactions in ZTC-3 are apparently a consequence of the confined pore geometry available for the adsorbed molecules. Alternatively, or perhaps in combination, the entropy of adsorption may increase with coverage more rapidly for ZTC-3 (the underlying changes in molecular dynamics could be studied with CD₄).

Accurate assessment of the contribution of intermolecular interactions to q_{st} requires knowledge about the adsorption energies of the different surface sites. The most favorable sites contribute to the adsorption at low coverage in the Henry's law regime, but a heterogeneity of site energies as in MSC-30 is reflected in the relatively rapid decrease of q_{st} with θ . The material properties of ZTC-3, such as a narrow distribution of pore width, periodic pore spacing, and high content of sp²-hybridized carbon (as characterized by NMR and numerous other techniques¹⁸), suggest a high homogeneity of binding site energies. We expect that the increase of 1.1 kJ/mol in q_{st} at 238 K reflects most of the contribution from favorable intermolecular interactions, and this increase is in good agreement with calculations of lateral interactions of methane molecules on a surface.^{14,21}

An isosteric enthalpy of adsorption that increases with θ over a large range of T and P is highly desirable for a methane adsorbent material. It benefits deliverable storage capacity because a large fraction of the maximum adsorption capacity occurs at pressures above the lower bound of useful storage rather than below it, as occurs for materials with a high initial binding energy that decreases with loading. Indeed, the deliverable gravimetric methane capacities of ZTC-3 at temperatures near ambient are the highest of any reported carbonaceous material (see SI). The flexibility of the template carbonization synthesis allows pore widths to be adapted to other adsorptive gases by simply changing the template, making this a promising approach for the design of adsorbent materials for other gases with attractive intermolecular interactions.

■ ASSOCIATED CONTENT

📄 Supporting Information

Experimental techniques, materials characterization, and thermodynamic model. This material is available free of charge via the Internet at <http://pubs.acs.org>.

■ AUTHOR INFORMATION

Corresponding Author

nstadie@caltech.edu

Notes

The authors declare no competing financial interest.

■ ACKNOWLEDGMENTS

We thank John Vajo and Robert Cumberland for discussions and materials synthesis. This work was supported as part of EFree, an Energy Frontier Research Center under Award No. DE-SG0001057.

■ REFERENCES

- (1) Zhou, Y.; Zhou, L. *Langmuir* **2009**, *25*, 13461.
- (2) Alcañiz-Monge, J.; Lozano-Castelló, D.; Cazorla-Amorós, D.; Linares-Solano, A. *Microporous Mesoporous Mater.* **2009**, *124*, 110.
- (3) Panella, B.; Hirscher, M.; Roth, S. *Carbon* **2005**, *43*, 2209.
- (4) Poirier, E.; Chahine, R.; Bose, T. K. *Int. J. Hydrogen Energ.* **2001**, *26*, 831.
- (5) Bhatia, S. K.; Myers, A. L. *Langmuir* **2006**, *22*, 1688.
- (6) Chung, T. C. M.; Jeong, Y.; Chen, Q.; Kleinhammes, A.; Wu, Y. J. *Am. Chem. Soc.* **2008**, *130*, 6668.
- (7) Jin, Z.; Sun, Z. Z.; Simpson, L. J.; O'Neill, K. J.; Parilla, P. A.; Li, Y.; Stadie, N. P.; Ahn, C. C.; Kittrell, C.; Tour, J. M. *J. Am. Chem. Soc.* **2010**, *132*, 15246.
- (8) Xia, Y.; Walker, G. S.; Grant, D. M.; Mokaya, R. *J. Am. Chem. Soc.* **2009**, *131*, 16493.
- (9) Lozano-Castello, D.; Cazorla-Amoros, D.; Linares-Solano, A.; Quinn, D. F. *Carbon* **2002**, *40*, 989.
- (10) Matranga, K. R.; Myers, A. L.; Glandt, E. D. *Chem. Eng. Sci.* **1992**, *47*, 1569.
- (11) Nicholson, D. *Carbon* **1998**, *36*, 1511.
- (12) Cracknell, R. F.; Gordon, P.; Gubbins, K. E. *J. Phys. Chem.* **1993**, *97*, 494.
- (13) Jin, Z.; Lu, W.; O'Neill, K. J.; Parilla, P. A.; Simpson, L. J.; Kittrell, C.; Tour, J. M. *Chem. Mater.* **2011**, *23*, 923.
- (14) Salem, M. M. K.; Braeuer, P.; Szombathely, M.; Heuchel, M.; Harting, P.; Quitzsch, K.; Jaroniec, M. *Langmuir* **1998**, *14*, 3376.
- (15) Bénard, P.; Chahine, R. *Langmuir* **2001**, *17*, 1950.
- (16) Nishihara, H.; Kyotani, T. *Adv. Mater.* **2012**, *24*, 4473.
- (17) Nishihara, H.; Hou, P. X.; Li, L. X.; Ito, M.; Uchiyama, M.; Kaburagi, T.; Ikura, A.; Katamura, J.; Kawarada, T.; Mizuuchi, K.; Kyotani, T. *J. Phys. Chem. C* **2009**, *113*, 3189.
- (18) Stadie, N. P.; Vajo, J. J.; Cumberland, R. W.; Wilson, A. A.; Ahn, C. C.; Fultz, B. *Langmuir* **2012**, *28*, 10057.
- (19) Voskuilen, T.; Pourpoint, T.; Dailly, A. *Adsorption* **2012**, *18*, 239.
- (20) Sun, Y.; Liu, C.; Su, W.; Zhou, Y.; Zhou, L. *Adsorption* **2009**, *15*, 133.
- (21) Sillar, K.; Sauer, J. *J. Am. Chem. Soc.* **2012**, 18354.
- (22) McNicholas, T. P.; Wang, A.; O'Neill, K.; Anderson, R. J.; Stadie, N. P.; Kleinhammes, A.; Parilla, P.; Simpson, L.; Ahn, C. C.; Wang, Y.; Wu, Y.; Liu, J. *J. Phys. Chem. C* **2010**, *114*, 13902.
- (23) Purewal, J. J.; Kabbour, H.; Vajo, J. J.; Ahn, C. C.; Fultz, B. *Nanotechnology* **2009**, *20*, 204012.
- (24) Stadie, N. P.; Purewal, J. J.; Ahn, C. C.; Fultz, B. *Langmuir* **2010**, *26*, 15481.
- (25) Mertens, F. O. *Surf. Sci.* **2009**, *603*, 1979.
- (26) Sircar, S. *Ind. Eng. Chem. Res.* **1999**, *38*, 3670.
- (27) Stadie, N. P. PhD. thesis, Caltech, 2012.
- (28) Myers, A. L.; Calles, J. A.; Calleja, G. *Adsorption* **1997**, *3*, 107.
- (29) Aranovich, G.; Donohue, M. *J. Colloid Interface Sci.* **1997**, *194*, 392.
- (30) Ono, S.; Kondo, S. *Molecular theory of surface tension in liquids*; Springer-Verlag: Berlin, 1960.
- (31) Saha, D.; Wei, Z.; Deng, S. *Int. J. Hydrogen Energ.* **2008**, *33*, 7479.
- (32) Aranovich, G. L.; Donohue, M. D. *Carbon* **1995**, *33*, 1369.
- (33) Purewal, J.; Liu, D.; Sudik, A.; Veenstra, M.; Yang, J.; Maurer, S.; Müller, U.; Siegel, D. J. *J. Phys. Chem. C* **2012**, *116*, 20199.
- (34) Sircar, S.; Mohr, R.; Ristic, C.; Rao, M. B. *J. Phys. Chem. B* **1999**, *103*, 6539.
- (35) Rouquerol, F.; Rouquerol, J.; Sing, K. S. W. *Adsorption by powders and porous solids: principles, methodology, and applications*; Academic Press: San Diego, 1999.
- (36) Al-Muhtaseb, S. A.; Ritter, J. A. *J. Phys. Chem. B* **1999**, *103*, 2467.